Anion Binding by Transferrins: Importance of Second-Shell Effects Revealed by the Crystal Structure of Oxalate-Substituted Diferric Lactoferrin † , ‡

ARTICLE *in* BIOCHEMISTRY · AUGUST 1996

Impact Factor: 3.02 · DOI: 10.1021/bi960288y · Source: PubMed

Articles

Anion Binding by Transferrins: Importance of Second-Shell Effects Revealed by the Crystal Structure of Oxalate-Substituted Diferric Lactoferrin[†,‡]

Heather M. Baker, Bryan F. Anderson, Andrew M. Brodie, Musa S. Shongwe, Clyde A. Smith, and Edward N. Baker*

Department of Chemistry and Biochemistry, Massey University, Palmerston North, New Zealand

Received February 7, 1996[⊗]

ABSTRACT: Proteins of the transferrin family bind, with high affinity, two Fe^{3+} ions and two CO_3^{2-} ions but can also bind other metal ions and other anions. In order to find out how the protein structure and its two binding sites adapt to the binding of larger anions, we have determined the crystal structure of oxalate-substituted diferric lactoferrin at 2.4 Å resolution. The final model has a crystallographic *R*-factor of 0.196 for all data in the range 8.0−2.4 Å. Substitution of oxalate for carbonate does not produce any significant change in the polypeptide folding or domain closure. Both binding sites are perturbed, however, and the effects are different in each. In the C-lobe site the oxalate ion is bound to iron in symmetric 1,2-bidentate fashion whereas in the N-lobe the anion coordination is markedly asymmetric. The difference arises because in each site substitution of the larger anion causes displacement of the arginine that forms one wall of the anion binding site; the movement is different in each case, however, because of different interactions with "second shell" amino acid residues in the binding cleft. These observations provide an explanation for the site inequivalences that accompany the substitution of non-native anions and cations.

Proteins of the transferrin family are known primarily for their metal binding ability. These proteins, which include serum transferrin, ovotransferrin, and lactoferrin, have the property of binding, very tightly but reversibly, two Fe^{3+} ions per molecule of protein (Brock, 1985; Harris & Aisen, 1989; Baker, 1994). In the case of transferrin at least, this is vital for the uptake of iron by animals and for the maintenance of proper levels of iron in body fluids.

The importance of anion binding by transferrins is less obvious but is highlighted by two observations. The first is that Fe^{3+} ions cannot be bound tightly without the concomitant binding of a suitable anion, normally CO_3^{2-}. This relationship between anion and cation is synergistic in the sense that each is required for tight binding of the other. Moreover, both kinetic and structural evidence suggests that the anion binds first and prepares the site for metal binding (Cowart *et al*., 1982; Kojima & Bates, 1981; Baker *et al*., 1987; Anderson *et al*., 1989). The second observation that focuses on the importance of anion binding is the structural and functional similarity between transferrins and certain bacterial anion binding proteins (Baker *et al*., 1987). The site occupied by carbonate in transferrins appears homologous with that occupied by sulfate and phosphate in bacterial periplasmic binding proteins, suggesting that transferrins could reasonably be thought of as anion binding proteins to which a metal binding functionality has been added (Baker, 1994).

The three-dimensional structures of both human lactoferrin (Anderson *et al*., 1987, 1989) and rabbit transferrin (Bailey *et al*., 1988) have been determined by X-ray crystallography. The proteins are bilobal, with the N-terminal half of the polypeptide forming one lobe (N-lobe) and the C-terminal half the other (C-lobe). In each lobe the combined metal and anion site is in a deep cleft between two domains (N1 and N2 in the N-lobe, C1 and C2 in the C-lobe). In the native proteins, with Fe^{3+} and CO_3^{2-} bound, the two sites are remarkably similar. In each case the metal ion is bound to the same four protein ligands (two Tyr, one His, one Asp) and the CO_3^{2-} ion bridges between the metal and the protein; it binds in symmetrical bidentate fashion to the Fe^{3+} ion and forms an exquisite set of hydrogen bonds with an anion binding site on the N2 (or C2) domain. This anion site is formed by the N-terminus of an α-helix (helix 5) and an arginine side chain.

Two intriguing questions are raised by the binding properties of transferrins. First, although Fe^{3+} and CO_3^{2-} are the preferred species bound, and are probably of the greatest physiological significance, many other metal ions and anions can also bind, apparently in the same sites. Among metal ions this includes many di- and trivalent transition metal ions, trivalent lanthanides, other trivalent cations such as Al^{3+} and Ga^{3+}, and even tetravalent actinides, Th^{4+} and Pu^{4+} (reviewed in Baker (1994)]. Likewise many other anions, most of them carboxylate ions (oxalate, malonate, glycolate, etc.), can substitute for carbonate under carbonate-free conditions (Schlabach & Bates, 1975; Baker,

[†] This research was supported by grants from the Health Research Council of New Zealand and the National Institutes of Health (HD20859 to E.N.B.). E.N.B. also receives research support as an International Research Scholar of the Howard Hughes Medical Institute.

[‡] The atomic coordinates have been deposited in the Brookhaven Protein Data Bank (filename 1BKA).

* To whom correspondence should be addressed. Phone: (64) (6) 350-5367. Fax: (64) (6) 350-5682. Email: T.Baker@massey.ac.nz.

[⊗] Abstract published in *Advance ACS Abstracts,* June 15, 1996.

S0006-2960(96)00288-7 CCC: $12.00

1994). The question of how these varying metal ions and anions are bound, and the extent to which they perturb the protein structure, is of fundamental importance to understanding their physiological significance. This is because the ultimate cellular fate of species bound to transferrins depends on receptor binding and hence on the protein conformation.

A second question of transferrin chemistry concerns the equivalence of the two sites. Although crystallographic studies show that the N- and C-lobe sites appear essentially identical, when Fe^{3+} and CO_3^{2-} are bound, many spectroscopic studies have shown marked inequivalences between the sites when other species are bound. For example, when Cr^{3+} is bound to either transferrin (Aisen *et al*., 1969) or lactoferrin (Ainscough *et al*., 1980) one Cr^{3+} ion is more readily displaced by Fe^{3+} than the other. Similarly, when Cu^{2+} is the metal ion in human lactoferrin (Ainscough *et al*., 1983), human serum transferrin (Zweier & Aisen, 1977), or ovotransferrin (Zweier, 1980), oxalate is bound preferentially in one site over the other. The origin of these inequivalences is unknown.

Given the importance of iron binding physiologically, and the prevalence of many different metabolites (oxalate, glycolate, etc.), which can act as synergistic anions, we present here the crystal structure of a complex of human lactoferrin in which oxalate is used as the synergistic anion, with Fe^{3+} as the associated cation. This complex, diferric dioxalatolactoferrin [$Fe_2(C_2O_4)_2Lf$], shows how the larger oxalate anion is accommodated in the binding cleft without disturbance of the overall polypeptide structure. It also reveals an unexpected difference in anion binding geometry between the two sites, and this has led, for the first time, to an explanation for the inequivalent behavior of the two sites in terms of the influence of more distant, "second shell", amino acid residues in the binding cleft.

MATERIALS AND METHODS

Experimental Procedures. All glassware was soaked in nitric acid and thoroughly rinsed with Milli-Q water prior to use, and all buffers were passed through a Bio-Rad Chelex 100 column, 100−200 mesh, to minimize contamination by adventitious metal ions.

UV−visible spectra in the range 250−700 nm were recorded using a Hewlett-Packard HP8452A diode array spectrophotometer. Electron paramagnetic resonance (EPR) spectra were recorded at 110 K, with protein concentrations of approximately 16 mg/mL, using a Varian E 104A spectrophotometer equipped with a Varian E257 variable temperature accessory. Spectral g values were calibrated with (diphenylpicryl)hydrazyl (DPPH) as a standard.

Rigorous exclusion of carbonate ions or carbon dioxide was achieved by using standard Schlenk-line techniques (Shriver, 1969). UV spectrophotometer measurements were carried out in dry, argon-filled 1.5 cm cuvettes sealed with rubber septa. EPR tubes were evacuated and back-filled with argon before use.

Preparation of $Fe_2(C_2O_4)_2Lf$. Human lactoferrin was prepared from fresh colostrum as described previously (Norris *et al*., 1989). This gave lactoferrin with a maximum iron content of 8−10% saturation, as estimated from the spectral ratios of A_{280nm}/A_{466nm} and A_{412nm}/A_{466nm} (Aisen & Leibman, 1972), compared with those of fully iron-saturated lactoferrin (ratios 20−23 and 0.70−0.75, respectively).

Table 1: Summary of Refinement

resolution range (Å)	8.0−2.4
no. of reflections	31758
R factor	0.196
protein atoms	5375
ions	$2Fe^{3+}$, $2C_2O_4^{2-}$
solvent molecules	121
RMS deviations from ideal values	
bond lengths (Å)	0.018
bond angle (1−3) distances (Å)	0.059
planes (Å)	0.011
chiral volumes (Å^3)	0.248
mean temperature factors (Å^2)	
main chain atoms	36.4
side chain atoms and solvent	40.4
Fe^{3+} ions	31.2, 28.0
$C_2O_4^{2-}$ ions	31.9, 20.8

Apolactoferrin (5 mL) (10 mg/mL, in 0.025 M Tris-HCl, 0.7 M NaCl, pH 8.0) was placed in a Schlenk tube, 6.3 mg of analytical reagent sodium oxalate (BDH) (50-fold excess) was dissolved in the solution, and the pH was gradually lowered to 4.3 with addition of 0.1 M metal-free HCl. Release of CO_2 was promoted by subjecting the solution to a small vacuum (10−12 mmHg) over a period of 2 h, during which time the Schlenk tube was intermittently flushed with argon. The pH was restored to 8.0 with CO_2-free NH_3. Using a spectrophotometer to monitor the titration, 2 μL aliquots of 0.01 M ferric nitrilotriacetate solution were then added to the oxalate/apolactoferrin solution until the saturation point was reached.

The resulting complex had a purple-red color, with a visible absorption maximum at 482 nm and a ratio A_{280nm}/A_{482nm} of 19.0. It was shown to have the EPR spectrum characteristic of the $Fe_2(C_2O_4)_2Lf$ complex (Shongwe *et al*., 1992), and this spectrum also confirmed the absence of any contamination by the corresponding carbonate complex.

Crystallization and Data Collection. As $Fe_2(C_2O_4)_2Lf$ slowly reverts to the carbonate complex in air, all buffers used for crystallization were subjected to the same repeated evacuation and flushing with argon as the protein solution. Purple-red, needle-shaped crystals, up to 1.2 × 0.6 × 0.6 mm in size, were grown at 4 °C by microdialysis of the protein solution (30 μL, 70 mg/mL protein) against 20 mL of 0.01 M sodium phosphate, pH 8.0, and 11% (v/v) methanol, in vials that had been back-filled with argon and sealed securely to prevent CO_2 contamination. The crystals were orthorhombic, $a = 155.5$ Å, $b = 96.9$ Å, $c = 55.85$ Å, and space group $P2_12_12_1$, with one molecule of $Fe_2(C_2O_4)_2$-Lf in the asymmetric unit.

X-ray diffraction data to 2.4 Å resolution were collected by screenless Weissenberg photography, using a Weissenberg camera equipped with imaging plates (Sakabe, 1991) at the Photon Factory synchrotron radiation source (Tsukuba, Japan). The camera radius was 430 mm, and the X-ray wavelength used was 1.0 Å. Two data sets were collected, one from a crystal mounted along its *a* axis and the other from a second crystal mounted along its *b* axis. In each case a rotation range exceeding 90° was covered; each image covered an oscillation range of 7.0°, with an overlap of 0.5° between successive images giving a total range of 98° for 15 images. Diffraction images were processed using the program WEIS (Higashi, 1989). From a total of 163 844

measured reflections, 31 758 unique reflections with $I > \sigma_I$ were obtained with an overall merging R value of 0.115. This represents a data set that was 94.9% complete to 2.4 Å resolution (83.3% complete in the outermost, 2.54−2.4 Å, shell, with 50% of the reflections in this shell having $I > 2\sigma_I$) (see Table 1).

Structure Determination and Refinement. The crystals of $Fe_2(C_2O_4)_2$Lf were isomorphous with those of native diferric lactoferrin, $Fe_2(CO_3)_2$Lf (Baker & Rumball, 1978). The refined diferric lactoferrin structure (Haridas *et al*., 1995) was therefore used as the starting model for refinement, after omission of the Fe^{3+} and CO_3^{2-} ions, the carbohydrate residues, all solvent molecules, and all protein side chains involved in metal and anion binding. The latter residues were all truncated at C_β, and all individual temperature factors were given an initial value of 25 Å^2. The initial R value was 0.34 for all data in the range 5.0−2.4 Å.

Crystallographic refinement was by restrained least squares using the fast Fourier version of PROLSQ (Hendrickson & Konnert, 1980). Restraints were applied to bond lengths, interbond angle distances, planar groups, nonbonded contact distances, and chiral volumes. Refinement proceeded in a series of rounds (of 20−30 cycles), during each of which restraints were loosened and then tightened again. Between rounds the model geometry was checked using the program PROCHECK (Laskowski *et al*., 1993), and manual rebuilding from $2F_o - F_c$ and $F_o - F_c$ "omit" maps was performed using the interactive graphics program FRODO (Jones, 1978). The Fe^{3+} ions and the metal ligands were added to the model when the R value was 0.29. After further refinement ($R = 0.28$) the two oxalate ions and their associated protein side chains (Thr 117 and Arg 121 in the N-lobe, Thr 461 and Arg 465 in the C-lobe) were built into well-defined electron density. Water molecules were added to the model when the R factor was below 0.25, but only where electron density was seen in both $2F_o - F_c$ and $F_o - F_c$ maps, at levels of 1σ and 3σ, respectively, and the positions made sense in terms of hydrogen-bonded contacts with neighboring atoms. Individual B values were assumed for all atoms when the R factor had dropped below 0.23. The solvent model was reevaluated on a number of occasions (leaving out all water molecules with $B > 60$ Å^2), and special attention was paid to the oxalate ions and associated protein groups which were examined a number of times through omit maps. No carbohydrate residues were included in the model; a diffuse area of positive density extended from the two glycosylation sites, Asn 137 and Asn 478, but it could not be interpreted in terms of individual sugar positions.

The final model comprises 5375 protein atoms (residues 4−691), 2 Fe^{3+} ions, 2 $C_2O_4^{2-}$ ions, and 121 solvent molecules, all treated as water. The R factor for this model is 0.196 for all measured X-ray data in the resolution range 8.0−2.4 Å (31758 reflections), with root-mean-square deviations from standard geometry of 0.018 Å (bond distances) and 0.059 Å (1−3 angle distances). A Ramachandran plot (Ramakrishnan & Ramachandran, 1965) of the main chain torsion angles (ϕ,ψ) shows that 82% of non-glycine residues are in the "most favored" regions defined in PROCHECK (Laskowski *et al*., 1993). There are only two outliers, Leu 299 and Leu 642, and as in other lactoferrin structures these have very well-defined electron density; their (ϕ,ψ) values are accounted for by the fact that each is the central residue in a γ-turn for which the normal (ϕ,ψ) values are around (70°, −50°) (Baker & Hubbard, 1984).

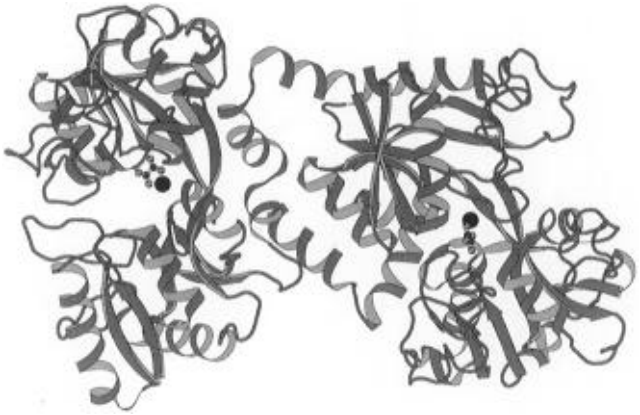

FIGURE 1: Polypeptide folding of $Fe_2(C_2O_4)_2$Lf, with the bound Fe^{3+} and $C_2O_4^{2-}$ ions shown in ball and stick representation. The N-lobe is to the left and C-lobe to the right. The figure was drawn with MOLSCRIPT (Kraulis, 1991).

RESULTS AND DISCUSSION

Polypeptide Folding. The polypeptide folding of $Fe_2(C_2O_4)_2$Lf is shown in Figure 1, in the form of a ribbon diagram. There are no significant conformational differences from that of native diferric lactoferrin (Haridas *et al*., 1995). In particular, substitution of the larger oxalate ion for carbonate in each lobe has not significantly altered the closure of the domains over the binding site. Superpositions of the $Fe_2(C_2O_4)_2$Lf structure onto the native $Fe_2(CO_3)_2$Lf show that the whole molecule superimposes with a root-mean-square deviation of 0.34 Å (687 C_α atoms, i.e., the whole polypeptide chain, omitting only the N-terminal residues 1−4, which are not included in the model). Superpositions of smaller components of the structure give root-mean-square deviations that are not significantly smaller: N-lobe, 0.34 Å (325 C_α); C-lobe, 0.32 Å (347 C_α); N1 domain, 0.34 Å (164 C_α); N2 domain, 0.29 Å (160 C_α); C1 domain, 0.33 Å (184 C_α); C2 domain, 0.28 Å (163 C_α). If the closures of the domains of each lobe are compared, as in Smith *et al*., (1994), the N-lobe of $Fe_2(C_2O_4)_2$Lf is 1.0° more open than that of $Fe_2(CO_3)_2$Lf and the C-lobe is 0.9° more open.

The above results show that binding of the larger oxalate ion in place of carbonate does not change the polypeptide conformation significantly, and any adjustments take place within the binding cleft. Comparisons of iron-bound and iron-free forms of lactoferrin (Anderson *et al*., 1990; Gerstein *et al*., 1993) show that large-scale conformational changes, involving rigid body domain rotations, accompany binding and release. As in copper-substituted lactoferrin (Smith *et al*., 1992) and a hybrid copper−carbonate/oxalate lactoferrin complex (Smith *et al*., 1994), however, the present structure shows that the domain closure hardly varies and must be determined primarily by the protein interfaces that are buried when closure takes place. The implications are that transferrins carrying ions other than Fe^{3+} and CO_3^{2-} could equally well be recognized by receptors.

Oxalate Binding. In both N-lobe and C-lobe binding sites the oxalate ion is bound to the Fe^{3+} ion in 1,2-bidentate fashion as in Figure 2. This provides direct crystallographic support for conclusions also reached from spectroscopic studies (Eaton *et al*., 1990; Dubach *et al*., 1991; Mangani &

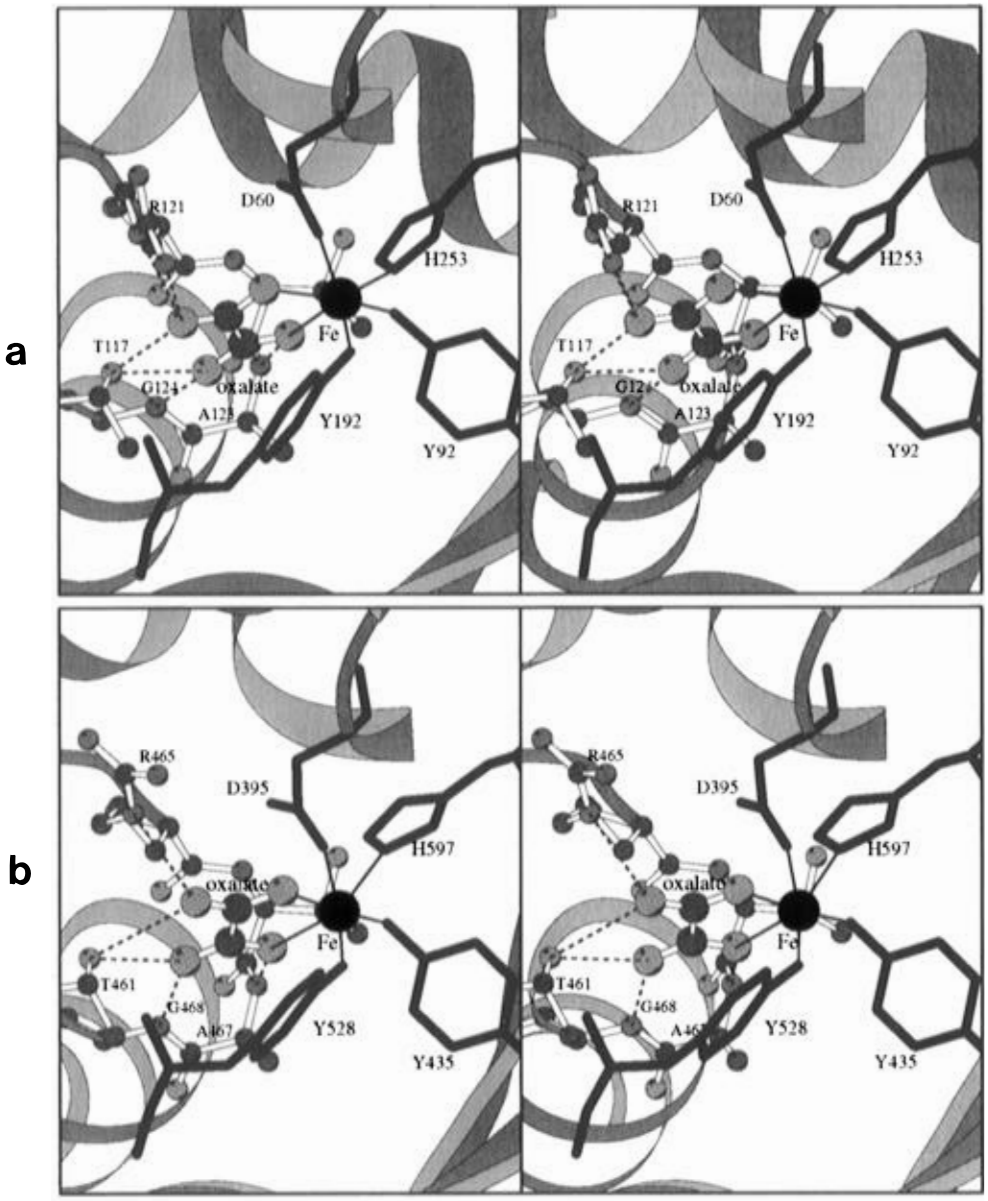

FIGURE 2: Stereo diagrams showing the oxalate binding in (a) the N-lobe and (b) the C-lobe of lactoferrin. Broken lines indicate hydrogen-bonding interactions with atoms of the anion binding site.

Messori, 1992). The oxalate ion also makes a series of hydrogen bonds with the residues that comprise the anion binding site on domain 2 of each lobe, in a way that closely resembles carbonate binding. One carboxylate group receives hydrogen bonds from peptide NH groups at the N-terminus of helix 5, together with the side chain OH of Thr 117 (or 461), and the other carboxylate receives hydrogen bonds from the arginine residue (121 or 465) which is present in almost all transferrins (Baker, 1994). These interactions are shown in Figure 2 and are listed in Table 2.

The original "interlocking sites" model for synergistic anion binding (Schlabach & Bates, 1975) proposed that anions bound to the metal through an electron donor group L and to a positively charged protein group through a carboxylate group. The crystal structure of a hybrid copper−carbonate/oxalate complex of lactoferrin led to an elaboration of this model, in which the carboxylate group of the synergistic anion binds to the N-terminus of a helix (helix 5) and metal coordination is through both a carboxylate oxygen and the adjacent electron donor group (Shongwe *et al*., 1992; Smith *et al*., 1994); the positively charged protein group, now identified as the arginine, may or may not hydrogen bond to the anion depending on the nature of the substituents on the anion. The present results show that this model (Figure 3) applies equally to both sites and is valid when Fe^{3+} is the metal ion, just as for Cu^{2+}.

Table 2: Bond Distances (Å) in Metal and Anion Sites

N-lobe		C-lobe	
Fe−$O_{\delta1}$(60)	1.91	Fe−$O_{\delta1}$(395)	1.98
Fe−O_{η}(92)	1.96	Fe−O_{η}(435)	1.83
Fe−O_{η}(192)	1.75	Fe−O_{η}(528)	1.81
Fe−$N_{\epsilon2}$(253)	2.13	Fe−$N_{\epsilon2}$(597)	2.32
Fe−O1(Ox)	1.87	Fe−O1(Ox)	2.07
Fe−O2(Ox)	2.55	Fe−O2(Ox)	1.91
O1(Ox)···N(123)	3.10	O1(Ox)···N(467)	2.88
O3(Ox)···N(124)	2.62	O3(Ox)···N(468)	2.98
O3(Ox)···$O_{\gamma1}$(117)	2.65	O3(Ox)···$O_{\gamma1}$(461)	2.69
O2(Ox)···$N_{\eta2}$(121)	2.51		
O4(Ox)···$N_{\eta2}$(121)	2.65		
O4(Ox)···N_{ϵ}(121)	2.51	O4(Ox)···N_{ϵ}(465)	2.89
O4(Ox)···$O_{\gamma1}$(117)	2.63	O4(Ox)···$O_{\gamma1}$(461)	3.40

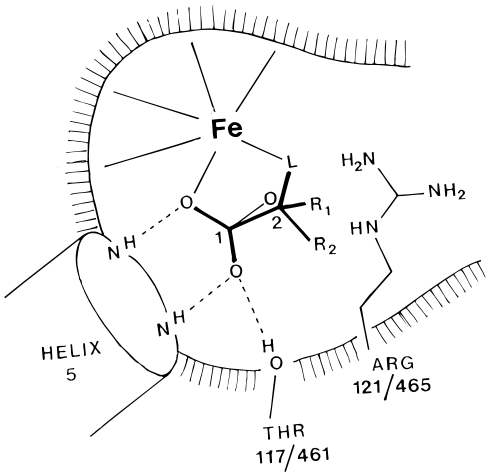

FIGURE 3: Generalized model for anion binding to transferrins based on the crystal structures of carbonate- and oxalate-substituted lactoferrins. Binding of a general anion (thick lines) compared with carbonate (thin lines) is shown. Adapted from Shongwe *et al.* (1992), with permission.

The larger size of the oxalate ion, compared with carbonate, results in some displacement of the arginine side chain, from its position in $Fe_2(CO_3)_2Lf$. This is achieved through small changes in the side chain torsion angles, $\chi_1-\chi_3$, in the order of 10−20°, which result in movement of the guanidinium group by 1.0 Å in the N-lobe and 2.9 Å in the C-lobe (measured as the displacement of C_ζ). This movement is made possible by the fact that, in $Fe_2(CO_3)_2Lf$, in the C-lobe Arg 465 makes no direct interactions with other protein groups, and in the N-lobe Arg 121 makes only one such contact (with Ser 191 OH); the rest of the interdomain cavity into which each arginine projects is filled with readily displaced water.

Displacement of the arginine side chain by oxalate does not abolish hydrogen bonding between it and the anion; in the N-lobe both N_ϵ and $N_{\eta 2}$ remain hydrogen bonded to the carboxylate group, as for carbonate, but in the C-lobe, where the displacement is greater, only N_ϵ remains hydrogen bonded. The stability of other anion complexes appears to correlate with the size of the anion and its ability to hydrogen bond to the arginine. Glycolate, glyoxylate, and thioglycolate, all of similar size to oxalate (two-carbon framework), cannot hydrogen bond to the arginine while remaining bidentate ligands to the metal and their complexes are less stable (Schlabach & Bates, 1975). Larger (three-carbon) anions give less stable complexes, but of these the most stable are malonate and α-ketomalonate, the only ones able to hydrogen bond with the arginine.

Differences between the Sites. The most striking difference between the sites is that in the C-lobe the oxalate binds in symmetrical bidentate fashion (Fe−O bond lengths of 1.91 and 2.07 Å) whereas in the N-lobe the binding is distinctly asymmetric (1.87 and 2.55 Å). Although the resolution of the X-ray analysis is only 2.4 Å, this difference is real; the oxalate positions were checked on a number of occasions during the refinement, through omit maps, and all attempts to impose the expected symmetric configuration on the N-lobe oxalate led to its returning to the asymmetric arrangement on further refinement. The consequences for the iron geometry are that both sites are distorted octahedral but that the long axis of the octahedron differs in each case. In the C-lobe it is the His 597 NE2−Fe−O1 (oxalate) axis

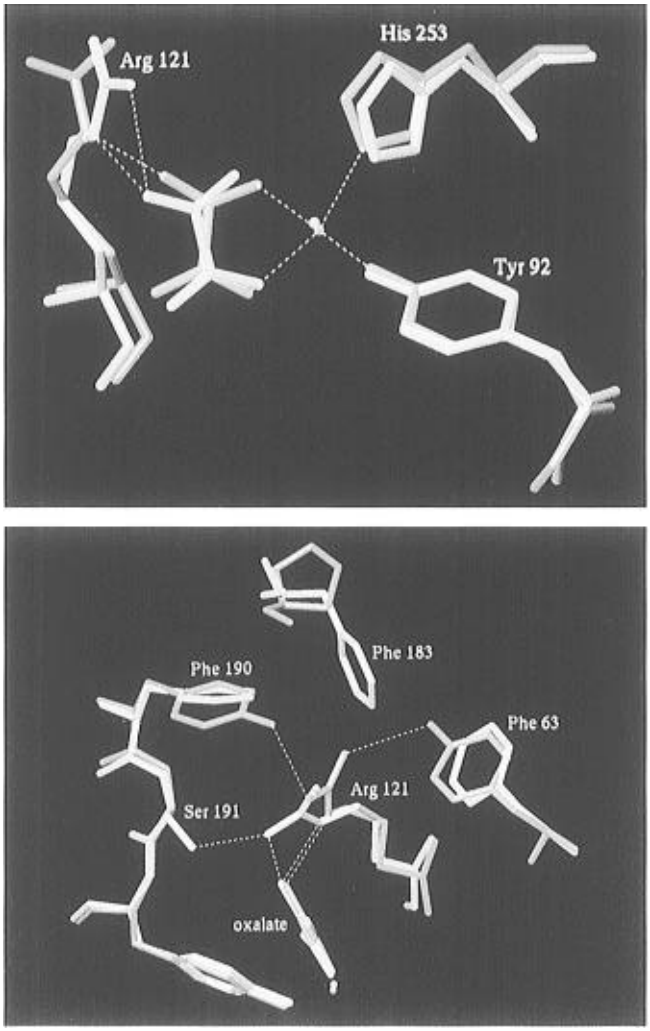

FIGURE 4: Superpositions of atoms of the N-lobe site (yellow) onto those of the C-lobe site (blue) in $Fe_2(C_2O_4)_2Lf$. In (a, top) the different orientations of the oxalate ions are shown. In (b, bottom) the greater movement of the C-lobe arginine (blue) and its different interactions can be seen. Bonded or hydrogen-bonded interactions are shown with broken lines. Residue numbers refer to the N-lobe; the equivalent C-lobe residues are given in the text.

(4.4 Å) whereas in the N-lobe it is the Tyr 92 OH−Fe−O2 (oxalate) axis (4.5 Å); the other axes are all in the order of 3.8 Å. This means that the site symmetries are different and must result in different spectroscopic signals.

The differences in oxalate coordination between the two sites are the first structural demonstration of the effects that have been noted in numerous spectroscopic studies when anions other than carbonate are bound. We are now in a position to examine the origin of these site inequivalences.

Superpositions of the atoms of the two binding sites (Figure 4) focus on the importance of second shell effects, due to residues beyond the immediate coordination environment. When the larger oxalate ion is bound, the arginine side chain is forced to move, but its movement is different in the two sites. In the C-lobe Arg 465 moves to a position in which it is stabilized by hydrogen bonds with Tyr 398 and Tyr 526 (Figure 4a), and this position is compatible with symmetric binding of the oxalate ion (which remains hydrogen bonded to the arginine). In the N-lobe no such stabilizing hydrogen bonds are possible as the equivalent second shell groups are Phe 63 and Phe 190. Moreover, the arginine, Arg 121, cannot move as far as Arg 465, both

because it is restrained by a hydrogen bond to Ser 191 and because it would clash with Phe 183 (equivalent to the much smaller Pro 519 in the C-lobe) and possibly also Phe 63 and Phe 190. The more restricted movement of Arg 121 then leads to a different orientation of the oxalate ion (Figure 4a) and asymmetric iron coordination.

The second shell residues, Phe 63, Phe 183, Phe 190, and Ser 191 in the N-lobe, and Tyr 398, Pro 519, Tyr 526, and Gly 527 thus exert different effects on the displaced arginines, through both steric and hydrogen-bonding interactions, and so indirectly determine the anion coordination. Moreover, if it is assumed that symmetric coordination is normally preferred by an oxalate ion, this explains why the C-lobe is the preferred site for oxalate binding by lactoferrin (because it can support symmetric binding).

The Metal−Anion Relationship. The synergistic relationship between metal ion and anion means that the effects of metal or anion substitution depend on the identity of the other ion. Thus, when Cu^{2+} is the metal ion, stable oxalate complexes of lactoferrin can be made by displacement of carbonate from $Cu_2(CO_3)_2$Lf (Shongwe *et al*., 1992). The corresponding oxalate complexes cannot be made by displacement when Fe^{3+} is the metal ion, however, and Fe^{3+}−oxalate complexes of lactoferrin are much more prone to reversion. In this context it is really the relative stabilities of oxalate and carbonate complexes that is relevant; since the binding site appears to be optimized for the geometrical requirements of Fe^{3+} and CO_3^{2-}, oxalate may not be able to compete well with carbonate when Fe^{3+} is the metal but can when Cu^{2+} is bound.

The differences in bonding accompanying metal and anion substitution are also emphasized by the visible absorption spectra of the carbonate and oxalate complexes. When Fe^{3+} is the metal ion, substitution of oxalate for carbonate shifts the visible charge transfer band to lower energy (466 to 482 nm), whereas when Cu^{2+} is the metal ion, the band is shifted in the opposite direction (434 to 420 nm) (Shongwe *et al*., 1992). The difference reflects the different types of metal orbitals involved. The visible charge transfer band is assigned as a phenolate $\pi \rightarrow$ metal d transition (Gaber *et al*., 1974; Ainscough *et al*., 1980), but the lowest available d orbital is of different type for the two metal ions; for d^5 Fe^{3+} it is d_{π^*} whereas for d^9 Cu^{2+} it is d_{σ^*}. The charge transfer transitions are thus phenolate(π) $\rightarrow$ Fe(d_{π^*}) and phenolate(π) $\rightarrow$ Cu(d_{σ^*}).

The difference between carbonate and oxalate is that oxalate is a stronger σ donor and weaker π donor than carbonate (Gray, 1965; Moeller, 1982). Thus when carbonate is replaced by oxalate, the metal d_{σ^*} orbitals are increased in energy (because d_σ are lowered) and d_{π^*} are decreased in energy (because d_π are increased). Thus oxalate substitution should cause a ligand $\rightarrow d_{\pi^*}$ transition (as for Fe^{3+}) to change to lower energy but a ligand $\rightarrow d_{\sigma^*}$ transition (as for Cu^{2+}) to increase in energy. This is as observed.

The substitution of oxalate for carbonate also affects the metal−tyrosine interaction. This is shown by the fact that the extinction coefficient for the charge transfer band is reduced by over 1000 mol^{-1} L cm^{-1}, going from $Fe_2(CO_3)_2$-Lf to $Fe_2(C_2O_4)_2$Lf (Shongwe *et al*., 1992), implying a weakened metal−Tyr interaction.

Conclusions. The structure revealed for the $Fe_2(C_2O_4)_2$-Lf complex shows that the lactoferrin molecule has sufficient *internal* flexibility to accept an oxalate ion in each site, in place of the preferred carbonate, without compromising its normal "closed" structure. The two sites respond differently, however, demonstrating the site inequivalences that arise when a nonpreferred species is bound; this has previously been seen also when Cu^{2+} is substituted for Fe^{3+} (Smith *et al*., 1992). What is clear in the present case is that the way in which each site responds depends on second shell effects, i.e., on residues beyond the immediate coordination sphere; these residues vary from one protein to another, making it likely that other transferrins may respond differently when larger anions are bound. The perturbations, structural and spectral, that are seen when oxalate is substituted also illustrate two key facts of transferrin chemistry. First, the binding sites are optimized for Fe^{3+} and CO_3^{2-}, and substitution of a different anion thus alters metal−anion, metal−tyrosine, and anion−protein interactions. Second, the weaker oxalate binding means that the precise mode of coordination is much more strongly influenced by the demands of the protein than is the case with carbonate.

ACKNOWLEDGMENT

We thank Professor Sylvia Rumball for her interest and encouragement, Dr. Eric Ainscough for helpful discussions regarding spectroscopy and bonding, and Richard Kingston and other members of the Protein Structural Laboratory for help with computing. We also gratefully acknowledge Dr. N. Sakabe and staff of the Photon Factory (Tsukuba, Japan) for making station 6A2 available to us and for help with the data collection.

REFERENCES

Ainscough, E. W., Brodie, A. M., Plowman, J. E., Bloor, S. J., Loehr, J. S., & Loehr, T. M. (1980) *Biochemistry 19*, 4072−4079.

Ainscough, E. W., Brodie, A. M., McLachlan, S. J., & Ritchie, V. S. (1983) *J. Inorg. Biochem. 18*, 103−112.

Aisen, P., & Leibman, A. (1972) *Biochim. Biophys. Acta 257*, 314−323.

Aisen, P., Aasa, A., & Redfield, A. G. (1969) *J. Biol. Chem. 244*, 4628−4633.

Anderson, B. F., Baker, H. M., Dodson, E. J., Norris, G. E., Rumball, S. V., & Baker, E. N. (1987) *Proc. Natl. Acad. Sci. U.S.A. 84*, 1769−1773.

Anderson, B. F., Baker, H. M., Norris, G. E., Rice, D. W., & Baker, E. N. (1989) *J. Mol. Biol. 209*, 711−734.

Anderson, B. F., Baker, H. M., Norris, G. E., Rumball, S. V., & Baker, E. N. (1990) *Nature (London) 344*, 784−787.

Bailey, S., Evans, R. W., Garratt, R. C., Gorinsky, B., Hasnain, S., Horsburgh, C., Jhoti, H., Lindley, P. F., Mydin, A., Sarra, R., & Watson, J. L. (1988) *Biochemistry 27*, 5804−5812.

Baker, E. N. (1994) *Adv. Inorg. Chem. 41*, 389−463.

Baker, E. N., & Rumball, S. V. (1977) *J. Mol. Biol. 111*, 207−210.

Baker, E. N., & Hubbard, R. E. (1984) *Prog. Biophys. Mol. Biol. 44*, 97−179.

Baker, E. N., Rumball, S. V., & Anderson, B. F. (1987) *Trends Biochem. Sci. 12*, 350−353.

Brock, J. H. (1985) in *Metalloproteins* (Harrison, P. M., Ed.) Part 2, pp 183−262, Macmillan Press, London.

Cowart, R. E., Kojima, N., & Bates, G. W. (1982) *J. Biol. Chem. 257*, 7560−7565.

Dubach, J., Gaffney, B. J., More, K., Eaton, G. R., & Eaton, S. S. (1991) *Biophys. J. 59*, 1091−1100.

Eaton, S. S., Dubach, J., Eaton, G. R., Thurman, G., & Ambruso, D. R. (1990) *J. Biol. Chem. 265*, 7138−7141.

Gaber, B. P., Miskowski, V., & Spiro, T. G. (1974) *J. Am. Chem. Soc. 96*, 6868−6873.

Gerstein, M., Anderson, B. F., Norris, G. E., Baker, E. N., Lesk, A. M., & Chothia, C. (1993) *J. Mol. Biol. 234*, 357−372.
Gray, H. B. (1965) *Electrons and Chemical Bonding*, W. A. Benjamin, New York.
Haridas, M., Anderson, B. F., & Baker, E N. (1995) *Acta Crystallogr. D51*, 629−646.
Harris, D. C., & Aisen, P. (1989) In *Iron Carriers and Iron Proteins* (Loehr, T. M., Ed.) pp 241−351, VCH Publishers, New York.
Hendrickson, W. A., & Konnert, J. H. (1980) In *Biomolecular Structure, Function, Conformation and Evolution* (Srinivasan, R., Ed.) Vol. 1, pp 43−57, Pergamon, Oxford.
Higashi, T. (1989) *J. Appl. Crystallogr. 22*, 9−18.
Jones, T. A. (1978) *J. Appl. Crystallogr. 11*, 268−272.
Kojima, N., & Bates, G. W. (1981) *J. Biol. Chem. 256*, 12034−12039.
Kraulis, P. J. (1991) *J. Appl. Crystallogr. 24*, 946−950.
Laskowski, R. A., MacArthur, M. W., Moss, D. S., & Thornton, J. M. (1993) *J. Appl. Crystallogr. 26*, 283−291.
Mangani, S., & Messori, L. (1992) *J. Inorg. Biochem. 46*, 1−6.
Moeller, T. (1982) *Inorganic Chemistry*, John Wiley, New York.
Norris, G. E., Baker, H. M., & Baker, E. N. (1989) *J. Mol. Biol. 209*, 329−331.
Ramakrishnan, C., & Ramachandran, G. N. (1965) *Biophys. J. 5*, 909−933.
Sakabe, N. (1991) *Nucl. Instrum. Methods Phys. Res. A303*, 448−463.
Schlabach, M. R., & Bates, G. W. (1975) *J. Biol. Chem. 250*, 2182−2188.
Shongwe, M. S., Smith, C. A., Ainscough, E. W., Baker, H. M., Brodie, A. M., & Baker, E. N. (1992) *Biochemistry 31*, 4451−4458.
Shriver, D. F. (1969) *The Manipulation of Air Sensitive Compounds*, McGraw-Hill, New York.
Smith, C. A., Anderson, B. F., Baker, H. M., & Baker, E. N. (1992) *Biochemistry 31*, 4527−4533.
Smith, C. A., Anderson, B. F., Baker, H. M., & Baker, E. N. (1994) *Acta Crystallogr. D50*, 302−316.
Zweier, J. L. (1980) *J. Biol. Chem. 255*, 2782−2789.
Zweier, J. L., & Aisen, P. (1977) *J. Biol. Chem. 252*, 6090−6096.

BI960288Y